Revue de Métallurgie **109**, 167–175 (2012)
© EDP Sciences, 2012
DOI: 10.1051/metal/2012020
www.revue-metallurgie.org

Revue de Métallurgie

Influence of parameters on microstructure of A356 alloy sheets processed by a novel rheo-rolling process

Ren-Guo Guan, Zhan-Yong Zhao, Chun-Guang Dai, Tong Cui and Qiu-Sheng Zhang

College of Materials and Metallurgy, Northeastern University, Shenyang 110004, China
e-mail: guanrg@smm.neu.edu.cn

Key words:
Semisolid; rheo-rolling; A356 alloy; microstructure; parameter

Received 16 November 2011
Accepted 27 April 2012

Abstract – A novel rheo-rolling process for producing A356 alloy sheet was developed. The influence of parameters on the microstructure of A356 alloy sheets was investigated. The eutectic fraction and primary α globule size increase with the increment in the roll speed. The globule size and eutectic fraction of A356 alloy sheet increase with the increment in the casting temperature. The primary α globule size decreases and the solid fraction increases with the increment in vibration frequency from 30 Hz to 80 Hz. With a roll speed of 0.069 m.s^{-1}, a casting temperature of 660 °C, and a vibration frequency of 80 Hz, A356 alloy sheet with a cross-section size of 4 × 160 mm was prepared. The microstructure is mainly composed of fine spherical or rosette α globules, and the average α globule size is 20.5 μm. The ultimate tensile strength of the A356 alloy sheet was 260 MPa, and the elongation to failure was 7.9%, which were 2.5 and 3.7 times greater than those of the as-cast material.

The rheo-rolling process was developed based on rolling and semisolid forming processes. Therefore, it has the following advantages [1–3]: firstly, due to the fact that the temperature of semisolid alloy is much lower than that of liquid alloy, the solidification time of semisolid alloy is shorter than that of liquid alloy, and the rolling speed can be improved greatly. Secondly, due to round solid α globules taking part in the deformation process during the rheo-rolling process, the mechanical properties of the products prepared by the rheo-rolling process are much higher than those prepared by the roll casting process [4, 5]. However, how to prepare good-quality semisolid slurry with low cost and high efficiency is an important subject for developing the rheo-rolling process. Therefore, many slurry preparation processes have been developed, such as Mechanical Stirring, Magnetohydrodynamic Stirring, Melt-Conditioned Direct-Chill Casting, Bubble Stirring, and so on [6–9]. As one of the slurry preparation processes, the sloping plate process has obvious advantages of high efficiency and low cost. This process involves casting liquid alloy onto a sloping plate, and the alloy is cooled and stirred by the cooling sloping plate, and then semisolid slurry with fine spherical primary α globules can be prepared. Many authors have also carried out research on this technique, such as Motegi, Kapranos, Grimmig and Haga et al. [10–14]. A semisolid rheo-rolling process was developed by combining the shape rolling mill with the vibrating sloping plate device to produce A356 alloy sheet. Since the product surface quality and properties of the sheet are related to its inner microstructure, and process parameters determine the inner microstructure of the sheet, the influence of parameters on the microstructure of A356 alloy sheets produced by the process was studied.

1 Materials and methods

The experimental equipment is the self-designed setup of the rheo-rolling process, as shown in Figure 1: the melt was cast onto the vibrating sloping plate, and the solid phase nucleated rapidly. The primary α globules grew into fine spherical structures

https://doi.org/10.1051/metal/2012020 Published online by Cambridge University Press
Article published by EDP Sciences

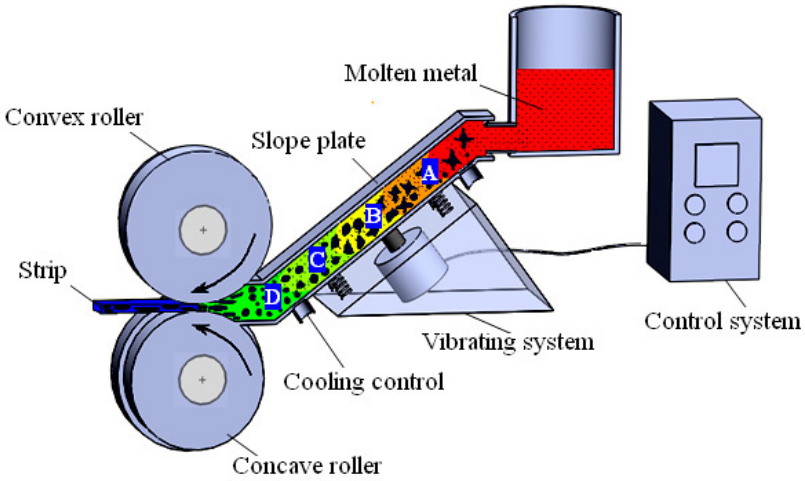


Fig. 1. The schematic diagram of the rheo-rolling process.

under the stirring action of vibrations and of the molten metal flow, making semi-solid processing feasible possible, and the slurry was rolled into shape by the rolling mill directly. The maximum diameter of the rolls is 400 mm. The rolls were cooled by circulating water. The cross-section size of the A356 alloy sheet is 4 × 160 mm. The experimental material was A356 alloy. The liquidus and solidus temperatures of the A356 alloy are about 615 °C and 577 °C. The chemical compositions (mass fraction, %) of the alloy are Si 7, Mg 0.4, Ti 0.1, Fe 0.12, Mn 0.05, Cu 0.1, Zn 0.05 and Al balanced.

The temperature of the semisolid slurry prepared by the sloping plate was measured by the thermocouple during the process. In order to study the effects of process parameters on the microstructure of A356 alloy sheets, the microstructures of the sheets produced under different process parameters were observed. The specimens were polished and etched by a solution of 40 ml HF + 760 ml H_2O, and the microstructures were observed under an OLYMPUS PMG51 metallographic microscope. The average α globule size was calculated by:

$$d = \frac{L_T}{N \times n} \tag{1}$$

where d is the average α globule size, L_T is the length of the measurement line, N is the α globule number that is covered by the measurement line, and n is magnification. A scanning electron microscope (SEM) was also used to analyze the distributions of alloy elements and the silicon morphology. The mechanical properties of the sheet were measured by using a CMT5105 tensile testing machine. The specimens are shown in Figure 2.

2 Results and discussion

2.1 Influence of roll speed on microstructure of A356 alloy sheet

The microstructures of A356 alloy on cross-sections of the sheet processed with different roll speeds are shown in Figure 3. Figure 4 shows the α globule size and solid fraction comparisons of the sheets produced under different roll speeds. The eutectic fraction and primary α globule size increase with the increment in the roll speed. The microstructure changes from the edges of the sheet in contact with the rolls to the central section of the sheet are not obvious, and the microstructure consists of spherical or rosette α globules. However, the solid fraction can be found to increase from the edges of the sheet to the central section of the sheet. The rolling speed influences the eutectic fraction that transformed from the liquid phase in the roll gap under rapid cooling.

Canyook et al. suggested that the heterogeneous nucleus on the plate surface and dendrite breakage caused microstructure refinement during the sloping plate

https://doi.org/10.1051/metal/2012020 Published online by Cambridge University Press

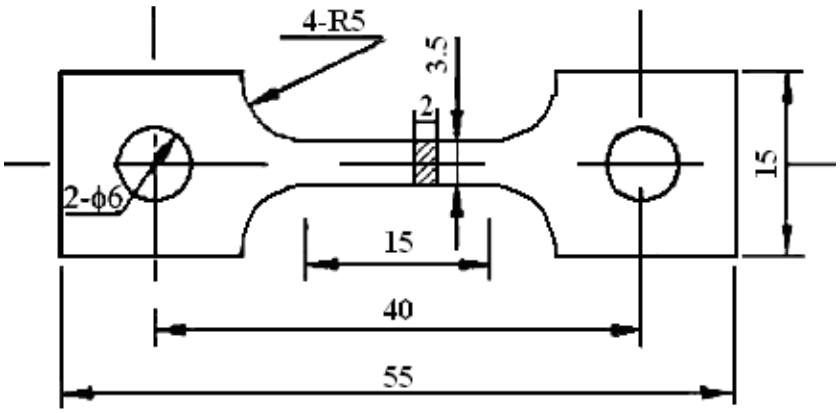


Fig. 2. Configuration of the samples used for the tensile tests (unit: mm).

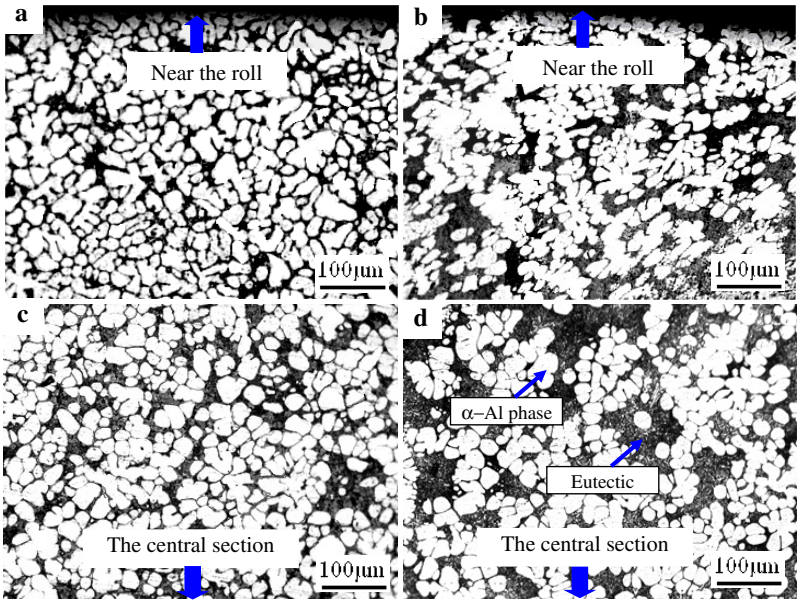


Fig. 3. The microstructures of A356 alloy sheets on cross-section under different roll speeds (the casting temperature is 680 °C, the vibration frequency is 60 Hz): (a), (c)-0.069 m.s^{-1}; (b), (d)-0.087 m.s^{-1}.

process [15]. In addition, recent studies found that the solute and temperature distributions in most of the melt are even; at the same time, the cooling rate of the melt on the sloping plate can reach 1000 K/s and is much greater than that of conventional casting. Therefore, eruptive nucleation can easily happen under these conditions. Heterogeneous nucleation and eruptive nucleation determine the microstructure of the sheet. When the roll speed was 0.087 m.s^{-1} and was relatively higher, the filling speed of the semisolid slurry was also higher, so the cooling time of the melt on the sloping plate and in the roll gap was shorter. The nucleation rate of the melt was correspondingly small. The second nucleation and crystallization of α-Al were not obvious under rapid cooling in the roll gap, so that the remaining liquid transformed into a eutectic aggregate. At the same time, the primary α globules ripened into large spherical or rosette structures. Therefore, the eutectic fraction and primary α globule size increase with the increment in the roll speed. When the roll speed was 0.069 m.s^{-1}, the α

https://doi.org/10.1051/metal/2012020 Published online by Cambridge University Press

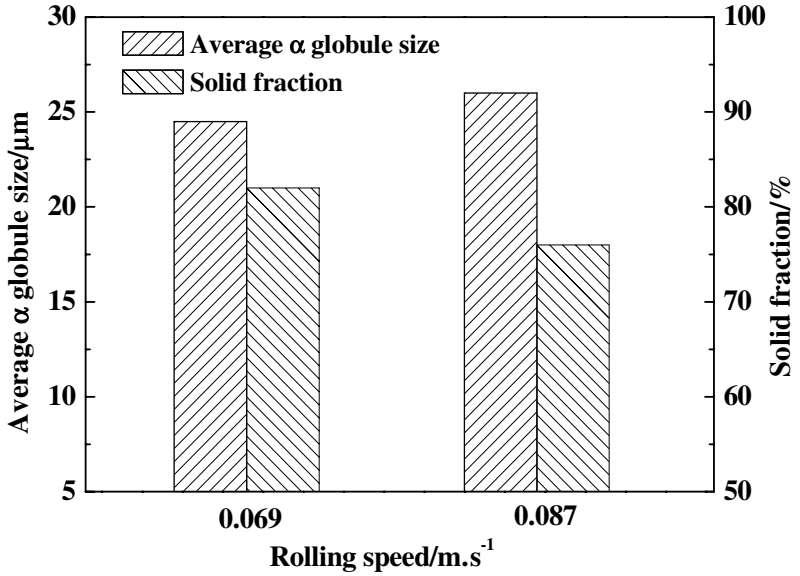


Fig. 4. The α-Al globule size and solid fraction produced under different roll speeds (the casting temperature is 680 °C, the vibration frequency is 60 Hz).

globule size and the eutectic fraction were correspondingly small. The optimized roll speed is 0.069 m.s^{-1}.

2.2 Influence of casting temperature on microstructure of A356 alloy sheet

Figure 5 shows the center microstructures of A356 alloy sheets on the cross-section for different casting temperatures. Figure 6 shows the relationship between the casting temperature, α globule size and solid fraction. The results reveal that the α globule size and eutectic fraction of A356 alloy sheet increase with the increment in casting temperature. When the casting temperature was 640 °C, the α globule size was 18.2 μm and the solid fraction was 88%, but the melt flow ability of the melt was very poor, and the process also failed. So, the casting temperatures were varied from 660 °C to 700 °C. When the casting temperature increases from 660 °C to 700 °C, the α globule size increases from 21 μm to 30 μm, and the solid fraction decreases from 84% to 75% correspondingly. When the casting temperature is higher than 680 °C, this tendency becomes more pronounced.

The nucleation rate of the alloy is greatly affected by casting temperature. The nucleation rate usually increases with the decrease in casting temperature. The second nucleation and crystallization of α-Al was not obvious in the roll gap under rapid cooling, and the residual liquids usually transformed into eutectic phases. The primary globule ripening happened mainly in the roll gap, so that the microstructure of the sheet was mainly determined by the nucleation rate of the semisolid slurry on the vibration sloping plate. Since the nucleation rate of the semisolid slurry increases with the decrease in casting temperature, the α globule size of the sheet also decreases with the decrease in casting temperature. When the casting temperature reached 700 °C, the nucleation rate on the sloping plate was reduced, and liquid fraction was too high. The residual liquid solidified rapidly with a eutectic structure rapidly in the roll gap, and large dendrites and eutectic structures were observed in the sheet, as shown in Figure 5d. SEM micrographs of the A356 sheet are shown in Figure 7. The eutectic Si becomes coarse with the increment in casting temperature gradually. When the casting temperature is 660 °C, the distribution of eutectic Si is homogeneous, and the eutectic Si is globular and very fine, much smaller than that of the sheet prepared at 680 °C. When the casting temperature was 660 °C, the temperature of the semisolid slurry prepared by the sloping

https://doi.org/10.1051/metal/2012020 Published online by Cambridge University Press

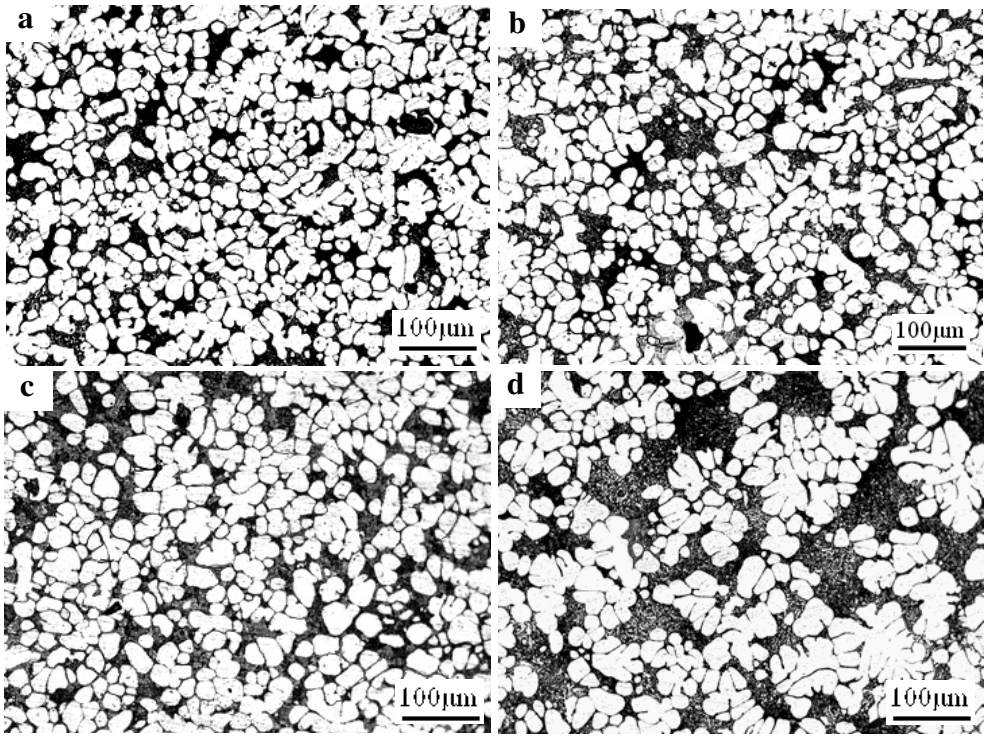


Fig. 5. The center microstructures of A356 alloy sheets on the cross-section under different casting temperatures (the roll speed is 0.069 m.s^{-1}, the vibration frequency is 70 Hz): (a)-640 °C; (b)-660 °C; (c)-680 °C; (d)-700 °C.

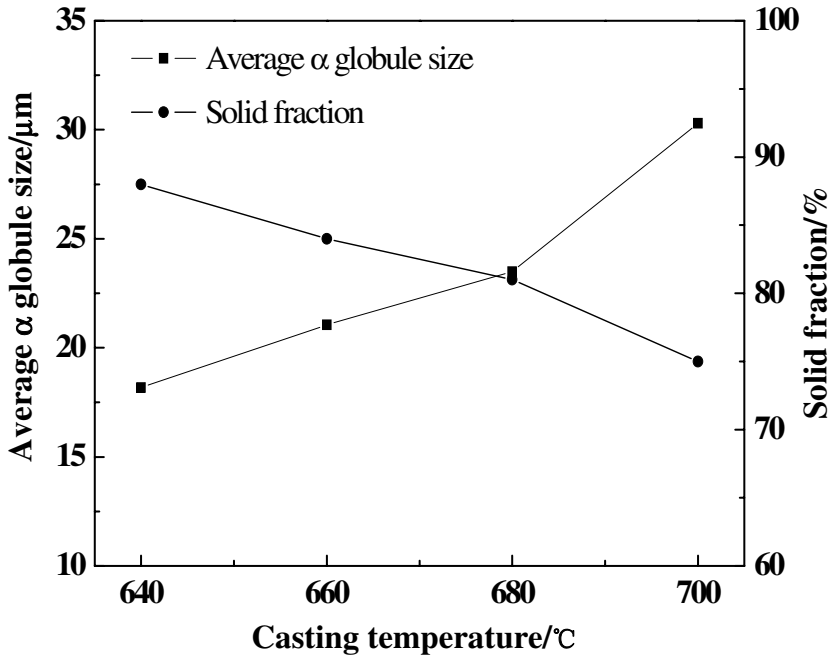


Fig. 6. Relationships of casting temperature, α globule size and solid fraction (the roll speed is 0.069 m.s^{-1}, the vibration frequency is 70 Hz).

https://doi.org/10.1051/metal/2012020 Published online by Cambridge University Press

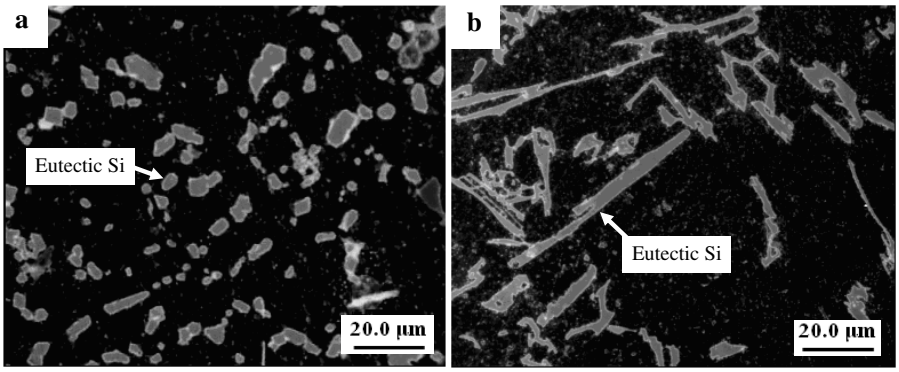


Fig. 7. The SEM images of the quenched semisolid slurry (the roll speed is 0.069 m.s^{-1}, the vibration frequency is 70 Hz): (a)-660 °C; (b)-680 °C.

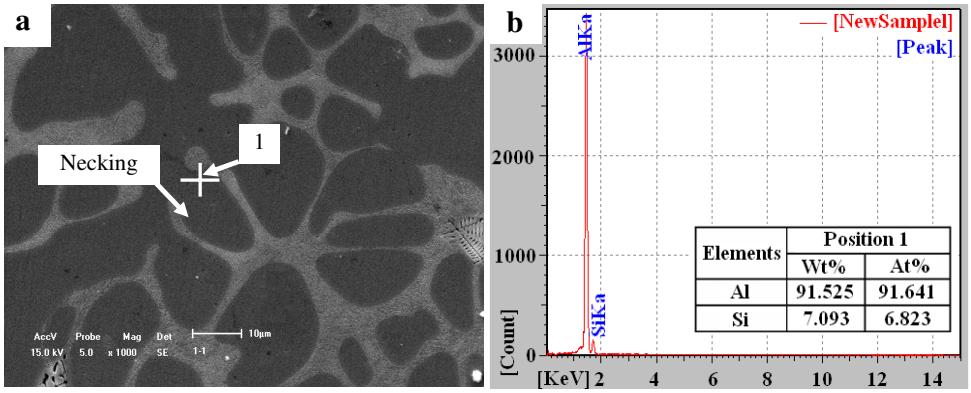


Fig. 8. The SEM images and the EDS analytical information of the quenched semisolid slurry (the casting temperature is 660 °C, the vibration frequency is 70 Hz).

plate was between about 580 °C and 600 °C. The SEM images and the EDS analytical information of the quenched semisolid slurry are shown in Figure 8. The aggregation of Si elements at the dendritic arm root can cause the corresponding areas to be weak, and these areas may neck down under heat flux and stirring easily. The dendritic arm fragments can grow further and evolve into fine spherical grains, which is favorable for rheo-rolling. So, a casting temperature at 660 °C is optimal.

2.3 Influence of vibrating frequency on microstructure of A356 alloy sheet

Vibration was applied on the sloping plate. Vibration can avoid slurry adhesion on the plate, accelerating the stirring of the melt, which is helpful to establish homogeneous solute and temperature fields and promotes eruptive nucleation. In addition, vibration can accelerate the dendrite breakage. Figure 9 shows the microstructures of A356 alloy sheet produced under different vibration frequencies. Figure 10 shows the average α globule size and solid fraction comparisons of the sheets produced under different vibration frequencies. The primary globule size decreases and the solid fraction increases with the increment in vibration frequency from 30 Hz to 80 Hz. The α globule size decreases from 27 μm to 20 μm, and the solid fraction increases from 81% to 88%. The α globule size is affected by the stirring strength of vibration. The stirring strength of vibration is determined by the dominant action of vibration frequency and amplitude. Vibration frequency mainly affects the cooling efficiency through the resulting good contact of the melt and the sloping plate,

https://doi.org/10.1051/metal/2012020 Published online by Cambridge University Press

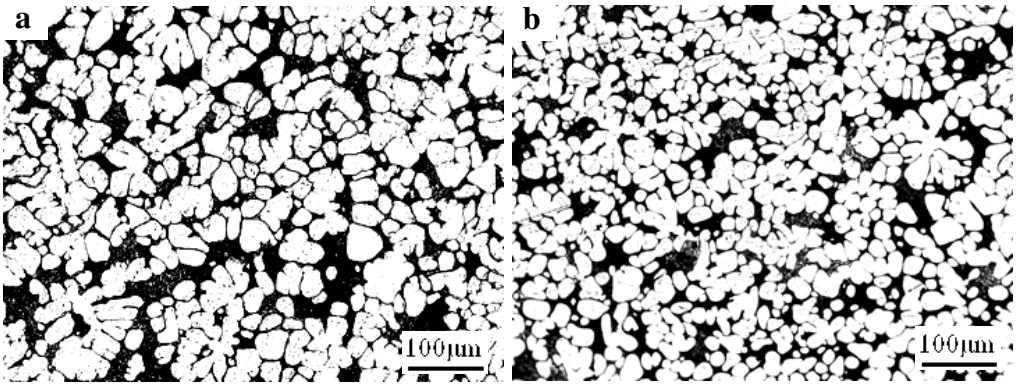


Fig. 9. The microstructures of A356 alloy sheet produced under different vibration frequencies (the casting temperature is 660 °C, the rolling speed is 0.069 m.s^{-1}): (a)-30 Hz; (b)-80 Hz.

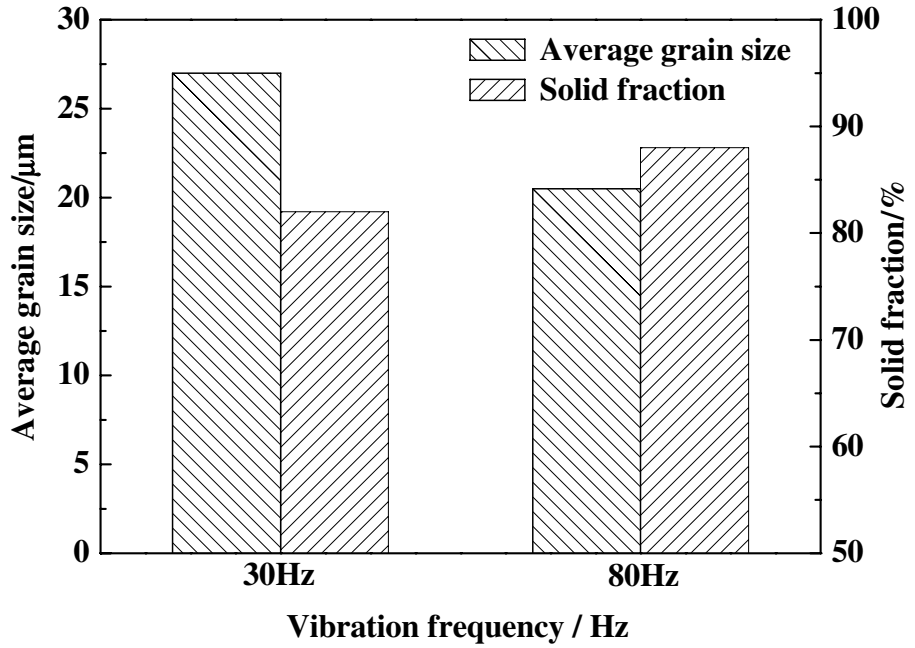


Fig. 10. The average α globule size and solid fraction comparisons of the sheets produced under different vibration frequencies (the casting temperature is 660 °C, the rolling speed is 0.069 m.s^{-1}).

Table 1. Relationship of vibration frequency and amplitude of the experimental device.

Vibration frequency, Hz	20	40	60	80	100
Vibration amplitude, mm	1.4	1.1	0.9	0.55	0.35

and the rate of the nuclei forming on the plate surface dispersing into the whole melt. This eventually affects the formation of a fine and spherical solid structure. Vibration amplitude mainly affects temperature and velocity distributions. With the increase in vibration intensity, it is more effective that the nuclei generated on the plate surface would be brought into the melt. What is more, the temperature and mass distribution become uniform, thus the dendritic formation and growth is depressed, which results in round and refined particles. The relationship of vibration frequency and amplitude of the experimental device is shown in Table 1. The vibration amplitude decreases with the in-

https://doi.org/10.1051/metal/2012020 Published online by Cambridge University Press

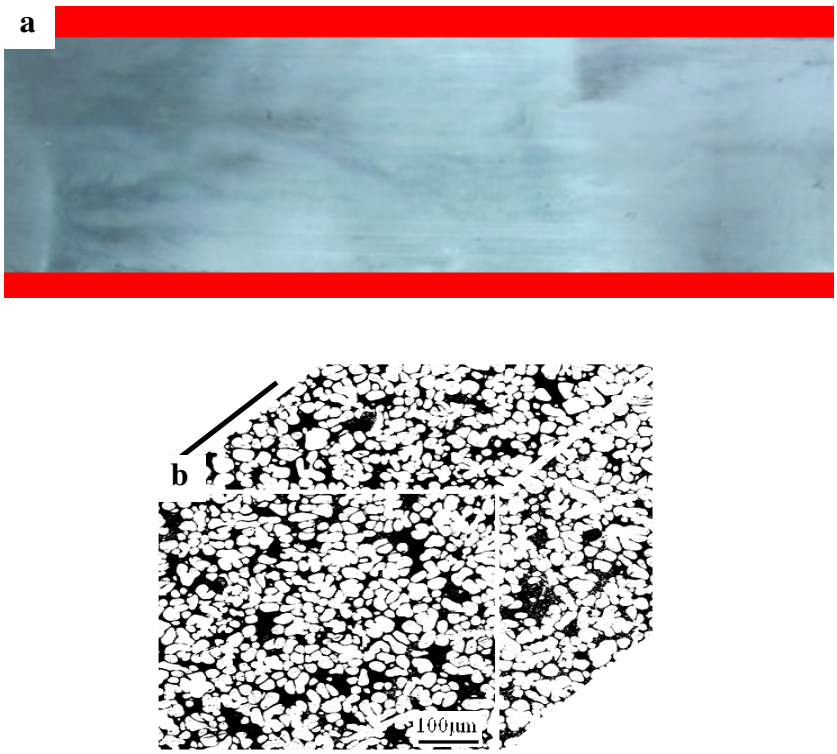


Fig. 11. A356 alloy sheet and its microstructure obtained: (a)-A356 alloy sheet; (b)-microstructure of the product.

crement in vibration frequency. When the vibration frequency is lower than 80 Hz, the frequency is the dominant factor that determines the stirring strength. But when the vibration frequency is higher than 80 Hz, the amplitude becomes the dominant factor that determines the stirring strength. When the frequency is 80 Hz, α globule size is relatively small. So, the proper vibration frequency is suggested to be 80 Hz.

With a roll speed of 0.069 m.s^{-1}, a casting temperature of 660 °C and a vibration frequency of 80 Hz, A356 alloy sheet with a cross-section size of 4 × 160 mm was prepared by the process, as shown in Figure 11a. The three-dimensional microstructure of the sheet is shown in Figure 11b. The microstructure is mainly composed of fine spherical or rosette globules, and the average α globule size of the sheet is 20.5 μm. The ultimate tensile strength of the A356 alloy sheet was 260 MPa, and the elongation to failure was 7.9%, as shown in Figure 12, which were 2.5 and 3.7 times greater than those of the as-cast material, respectively [16]. Additionally, the sheet produced by the rheo-rolling usually needs deep rolling, so the final properties could be improved significantly.

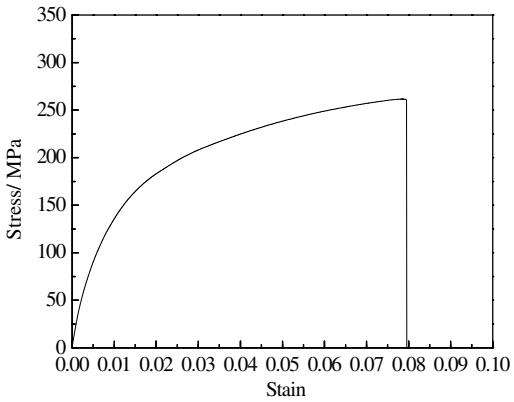


Fig. 12. Stress-strain curve of the A356 alloy sheet.

3 Conclusions

A novel rheo-rolling process for producing A356 alloy sheet was developed and optimized with a rolling speed of 0.069 m.s^{-1},

https://doi.org/10.1051/metal/2012020 Published online by Cambridge University Press

a casting temperature of 660 °C and a frequency of 80 Hz for an A356 alloy sheet with a cross-section size of 4 × 160 mm. The microstructure is mainly composed of fine spherical or rosette α-Al globules, and the average globule size is 20.5 μm. The ultimate tensile strength of the A356 alloy sheet was 260 MPa, and the elongation to failure was 7.9%, which were 2.5 and 3.7 times greater than those of the as-cast material, respectively. The eutectic fraction and primary α globule size increase with the increment in the roll speed. The α globule size and eutectic fraction increase with the increment in casting temperature. The primary globule size decreases and the solid fraction increases with the increment in vibration frequency from 30 Hz to 80 Hz.

Acknowledgements

The authors gratefully acknowledge the support of the National Natural Science Foundation of China under grants 51034002, 50974038 and 51074049, the Fok Ying Tong Education Foundation under grant 132002, and the Chinese National Program for Fundamental Research and Development under grant 2011CB610405.

References

[1] M.C. Flemings, *Metall. Mater. Trans. A* **22** (1991) 957-981

[2] Z.S. Zhen, W.M. Mao, S.J. Yan, A.M. Zhao, C.L. Cui, X.Y. Zhong, *Acta Metallurgica Sinica* **15** (2002) 505-510

[3] T. Rzychoñ, A. Kiełbus, *Archives Metall. Mater.* **53** (2008) 901-907

[4] R. Wechsler, *Revue de Métallurgie* **99** (2002) 941-948

[5] C. Hendricks, W. Rasim, H. Janssen, H. Schnitzer, E. Sowka, P. Tesè, *Revue de Métallurgie* **98** (2001) 655-666

[6] S. Ji, Z. Fan, M.J. Bevis, *Mater. Sci. Eng. A* **299** (2001) 210-217

[7] S.P. Midson, *Die Casting Engineer* **50** (2006) 48-51

[8] S. Ji, Z. Fan, *Metall. Metall. Trans. A* **33** (2002) 3511-3520

[9] J. Wannasin, R.A. Martinez, M.C. Flemings, *Diffusion and Defect Data Part B (Solid State Phenomena)* **116-117** (2006) 366-369

[10] T. Motegi, *Int. J. Mater. Product Technol.* **2** (2001) 468-475

[11] P. Kapranos, T. Haga, E. Bertoli, A. Pola, Z. Azpilgain, I. Hurtado, *Diffusion and Defect Data B (Solid State Phenomena)* **141-143** (2008) 115-120

[12] T. Grimmig, A. Ovcharov, C. Afrath, M. Bunck, A. Buhrig-Polaczek, *Diffusion and Defect Data Part B* (*Solid State Phenomena)* **116-117** (2006) 484-489

[13] T. Haga, K. Takahashi, M. Ikawaand, H. Watari, *J. Mater. Proc. Technol.* **153-154** (2004) 42-47

[14] R.G. Guan, Z.H. Xing, L. Shi, C. Wang, Y. Wang, *Materials Science Forum* **561-565** (2007) 865-868

[15] R. Canyook, S. Petsut, S. Wisutmethangoon, M.C. Flemings, J. Wannasin, *Trans. Nonferrous Metals Society of China* **20** (2010) 1649-1655

[16] R. Jamaati, S. Amirkhanlou, M.R. Toroghinejad, B. Niroumand, *Mater. Sci. Eng. A* **528** (2011) 2495-2510

https://doi.org/10.1051/metal/2012020 Published online by Cambridge University Press